ANTIOXIDANTS & REDOX SIGNALING
Volume 15, Number 12, 2011

DOI: 10.1089/ars.2011.4192

Mitochondrially Targeted α-Tocopheryl Succinate Is Antiangiogenic: Potential Benefit Against Tumor Angiogenesis but Caution Against Wound Healing

Jakub Rohlena,[1,*] Lan-Feng Dong,[2,*] Katarina Kluckova,[1] Renata Zobalova,[1,2] Jacob Goodwin,[2] David Tilly,[3] Jan Stursa,[3,4] Alena Pecinova,[5] Anatoly Philimonenko,[6] Pavel Hozak,[6] Jaideep Banerjee,[7] Miroslav Ledvina,[4] Chandan K. Sen,[7] Josef Houstek,[5] Mark J. Coster,[3] and Jiri Neuzil[1,2]

Abstract

Aims: A plausible strategy to reduce tumor progress is the inhibition of angiogenesis. Therefore, agents that efficiently suppress angiogenesis can be used for tumor suppression. We tested the antiangiogenic potential of a mitochondrially targeted analog of α-tocopheryl succinate (MitoVES), a compound with high propensity to induce apoptosis. ***Results:*** MitoVES was found to efficiently kill proliferating endothelial cells (ECs) but not contact-arrested ECs or ECs deficient in mitochondrial DNA, and suppressed angiogenesis *in vitro* by inducing accumulation of reactive oxygen species and induction of apoptosis in proliferating/angiogenic ECs. Resistance of arrested ECs was ascribed, at least in part, to the lower mitochondrial inner transmembrane potential compared with the proliferating ECs, thus resulting in the lower level of mitochondrial uptake of MitoVES. Shorter-chain homologs of MitoVES were less efficient in angiogenesis inhibition, thus suggesting a molecular mechanism of its activity. Finally, MitoVES was found to suppress HER2-positive breast carcinomas in a transgenic mouse as well as inhibit tumor angiogenesis. The antiangiogenic efficacy of MitoVES was corroborated by its inhibitory activity on wound healing *in vivo*. ***Innovation and Conclusion:*** We conclude that MitoVES, a mitochondrially targeted analog of α-tocopheryl succinate, is an efficient antiangiogenic agent of potential clinical relevance, exerting considerably higher activity than its untargeted counterpart. MitoVES may be helpful against cancer but may compromise wound healing. *Antioxid. Redox Signal*. 15, 2923–2935.

Introduction

CANCER IS A PATHOLOGY with a rather grim prognosis (20). This warrants the design and application of efficient new anticancer drugs acting *via* invariant targets that would allow broad applicability in different types of cancer. Mitochondria, an indispensable source of energy for most living cells, are increasingly recognized as such targets (12, 18, 24, 43). In this context, agents with anticancer activity acting on mitochondria, termed mitocans, present an intriguing group of compounds with relatively good selectivity for cancer cells (16, 27, 31). Mitocans are classified into eight groups, according to their mode of action (26). Vitamin E (VE) analogs belonging to group 5 mitocans act on the mitochondrial electron redox chain. These compounds are epitomized by the redox-silent α-tocopheryl succinate (α-TOS), an agent with high apoptogenic activity and selectivity for cancer cells (26, 30, 32). α-TOS has been shown to suppress a variety of tumors in mouse models, such as colorectal, breast (including HER2-positive tumors),

Innovation

The findings of this report show the very strong antiangiogenic activity of an analog of VE, α-TOS, tagged by addition of a TPP^+ group to localize to mitochondria. This endows the agent, MitoVES, with a particularly strong proapoptotic activity toward proliferating but not quiescent ECs, a paradigm that is helpful against tumor angiogenesis but may complicate wound angiogenesis and wound healing.

[1]Molecular Therapy Group, Institute of Biotechnology, Academy of Sciences of the Czech Republic, Prague, Czech Republic.
[2]School of Medical Science, Griffith University, Southport, Queensland, Australia.
[3]Eskitis Institute for Cell and Molecular Therapies, Griffith University, Nathan, Queensland, Australia.
Institutes of [4]Organic Chemistry and Biochemistry, [5]Physiology, and [6]Molecular Genetics, Academy of Sciences of the Czech Republic, Prague, Czech Republic.
[7]Davis Heart and Lung Research Institute, Ohio State University, Columbus, Ohio.
*These two authors contributed equally to this work.

mesothelioma, prostate, and pancreatic cancer as well as melanomas (22, 23, 40, 42, 45, 47).

Anticancer drugs can exert their activity *via* several modes of action. Most agents act by direct killing of malignant cells. However, an intriguing option to promote suppression of tumors is to starve them of energy and oxygen, that is, suppress the process of neovascularization of tumors by inhibiting angiogenesis (14). The process of neovascularization is based either on sprouting of new blood vessels from preexisting vessels (15) or on recruitment and differentiation of endothelial progenitor cells (35). It has been reported that angiogenesis can be suppressed by interfering with processes essential for its promotion and maintenance, in particular, disrupting paracrine signaling between tumor cells and endothelial cells (ECs) (3). This has been shown also for α-TOS, interfering with the generation and secretion of mitogenic cytokines such as the fibroblast growth factor-2 by malignant cells (29, 40).

Another possibility to suppress angiogenesis is the induction of apoptosis selectively in proliferating ECs. Several agents have been reported to possess such activity, including an analog of arsenite oxide (5) and α-TOS (10), consistent with the notion that targeting mitochondria of proliferating ECs is also an efficient way to suppress angiogenesis. Moreover, these results suggest that agents such as arsenites or α-TOS will efficiently kill angiogenic ECs of tumorigenic blood vessels while being nontoxic to the arrested ECs of normal blood vessels (33).

We have recently synthesized novel analogs of α-TOS that are targeted to mitochondria, more specifically to the interface of the matrix and the mitochondrial inner membrane (MIM). This mitochondrially targeted analog of α-TOS, MitoVES, is superior to its untargeted counterpart α-TOS in apoptosis induction and cancer suppression (7, 8). In this communication, we investigated whether MitoVES efficiently and selectively kills angiogenic ECs. The results indicate that MitoVES is much more efficient in angiogenic EC killing than the parental untargeted compound α-TOS, owing to the greater mitochondrial inner transmembrane potential ($\Delta\Psi_{m,i}$) of the proliferating EC, which translates to suppression of tumor progression and angiogenesis in an *in vivo* model of breast cancer.

Results

We first studied whether exposure of ECs to MitoVES (for its structure, see Fig. 1, where MitoVES is termed Mito$VE_{11}S$) results in apoptosis induction in the cells based on their proliferative status. For this, cells were seeded at two different confluencies, ~50%, with high proliferative status, and 100%, at which majority of the cells is growth arrested in G0. The proliferative status is documented by cell-cycle analysis, revealing majority of the proliferating ECs in the S phase, whereas confluent ECs were found mostly arrested in G0 (Fig. 2A, inset). Proliferating cells were susceptible to MitoVES, with almost all cells in apoptosis after 24-h exposure to 5 μM MitoVES. On the other hand, confluent ECs were highly resistant to the agent with substantial apoptosis (reaching ~40%) only at the highest concentration of MitoVES and at the longest exposures tested (Fig. 2A). Similarly, we observed accumulation of reactive oxygen species (ROS) in proliferating ECs exposed to MitoVES, whereas there was hardly any detectable increase in the level of ROS in confluent cells exposed to the agent (Fig. 2B). To see whether ROS generation and apoptosis induction in proliferating ECs exposed to MitoVES are causally linked, we treated the cells with the agent in the presence of a mitochondrially targeted analog of coenzyme Q (MitoQ) (21, 25). Data in Figure 2C and D document that the presence of the mitochondrially targeted antioxidant MitoQ suppressed both apoptosis induction and ROS accumulation in proliferating ECs, thus strongly indicating that ROS are important for the induction of apoptosis. We also exposed proliferating ECs to VES4TPP, an analog of MitoVES in which the triphenyl phosphonium (TPP^+) group was attached to the free succinyl group of the agent *via* a 4-C spacer (Fig. 1), which caused only minimal apoptosis (not shown). This indicates the importance of the free carboxylate for the apoptosis-inducing effects of the drug and shows that the correct placing of the TPP^+ targeting group is essential. In addition, it also demonstrates that the TPP^+ group without the active compound does not have any perceptible proapoptotic activity.

To get a better proof for the resistance of growth-arrested ECs to MitoVES, we tested whether the agent disrupts the contacts between individual cells. To do this, we plated the cells so that they reached 100% confluency, following which the cells were left untreated or exposed to 5 μM MitoVES for 20 h. At this point, the cells were either photographed in a light microscope or, after staining with anticadherin VE IgG plus secondary FITC-conjugated antibody and DAPI, observed in a confocal microscope. As shown in Figure 2E, the MitoVES-exposed cells maintained their normal morphology and their cell-to-cell contacts, indistinguishable from the control cells, thus further documenting the resistance of arrested ECs to MitoVES.

We tested the effect of MitoVES on angiogenesis *in vitro* by using two assays. First, we applied the wound-healing assay. ECs were allowed to form a fully confluent monolayer, after which a strip of cells was removed, and the wound was allowed to heal. Images in Figure 3A document that although at 20 h the denuded region completely filled with cells that either proliferated or migrated, 5 μM MitoVES prevented the process. The effect of MitoVES was concentration dependent, as documented in Figure 3B, showing the healing curves at different MitoVES levels. We calculated the healing rates from these curves and plotted them against different concentrations of MitoVES. Data in Figure 3C show that the healing rate of ~35 μm/h for untreated cells was suppressed to almost 5 μm/h in the presence of 5 μM MitoVES. This is reflected by the level of apoptosis in the healing assays, which was lowest in control cells and highest at 5 μM MitoVES (Fig. 3D).

The second angiogenesis assay *in vitro* is based on the tube-forming capacity of EAhy926 cells in a three-dimensional setting. Figure 3E documents the number of capillaries formed when the cells were seeded on Matrigel in the absence and presence of 5 μM MitoVES. Evaluation of the number of tubes revealed a dose-dependent inhibitory effect of MitoVES, with some 20 tubes per field for control cells and less than 3 tubes for cells exposed to 5 μM MitoVES (Fig. 3F). After retrieval of the treated cells from Matrigel, we estimated the level of apoptosis and found that the inhibitory activity of MitoVES on the tube-forming activity of the EAhy926 is directly proportional to the apoptosis-inducing efficacy of the agent (Fig. 3G).

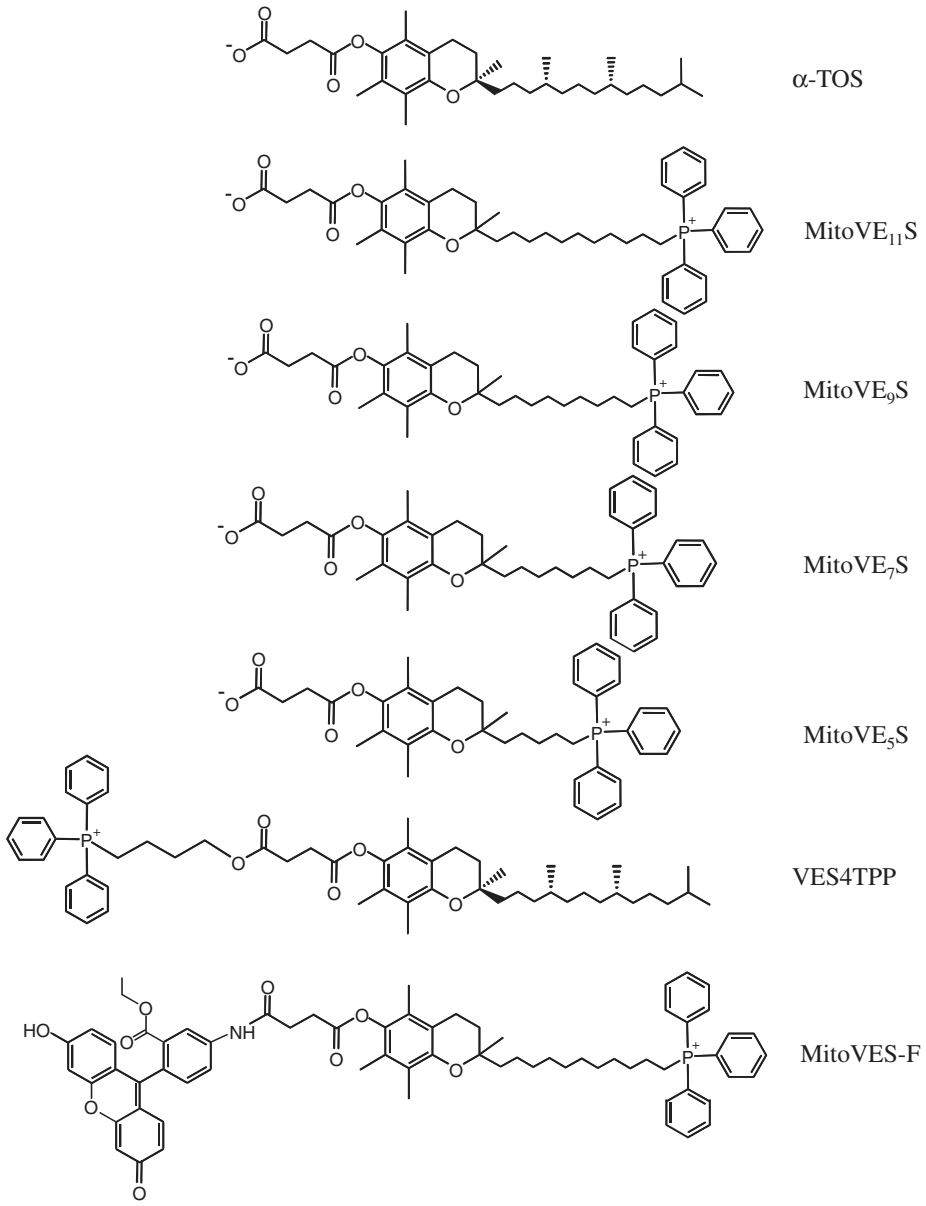

FIG. 1. Structures of the compounds used in the study. The structures shown are those of mitochondrially targeted analog of the vitamin E (VE) analog α-tocopheryl succinate (MitoVES) homologs that were used in the study and the mitochondrially untargeted analog, α-tocopheryl succinate (α-TOS).

We next tested the effect of MitoVES on angiogenesis *in vivo*, using the model of chronic ischemic wound employing the Laser Doppler blood flow imager (2, 36). In this model, proliferation of ECs is necessary to re-establish blood flow in the wounded area. Figure 4A documents that the agent at 20 μM inhibited the blood flow by $\sim$40%. Figure 4B shows representative images of control mice and mice treated with MitoVES. These results extend the previous *in vitro* anti-angiogenesis effect to an *in vivo* model.

Previous data indicate that mitochondria are important for the effect of MitoVES on proliferating ECs as indicated, in particular, by the protective effect of MitoQ. This can be expected due to the analogy of the mode of activity of MitoVES to that of α-TOS (46) and due to the mitochondrial targeting of the agent. To get stronger evidence, we tested mtDNA-depleted (ρ^0) EAhy926 cells for the effects of MitoVES on angiogenesis *in vitro* by using the wound-healing assays. We found that the ρ^0 EAhy926 cells are endowed with lower wound-healing activity compared with their parental counterparts. On the other hand, the wound-healing activity was strongly inhibited in the parental cells by MitoVES, whereas there was hardly any effect of the agent on the ρ^0 ECs (Fig. 5A, B). This resistance of the mtDNA-depleted ECs is likely due to their resistance to apoptosis induced in the assays by MitoVES (Fig. 5C). These results strongly point to the role of mitochondria in the effects of MitoVES on ECs just mentioned.

Mitochondrial localization of MitoVES is deduced from its chemistry, that is, tagging the VE analog with the cationic TPP^+ group and from its analogous structure to that of MitoQ (21, 25). To prove this supposition, we prepared a fluorescent analog of MitoVES by the addition of 5-aminofluorescein to the free carboxylate of MitoVES. Eahy926 cells, both proliferating and confluent, were then treated with fluorescently tagged MitoVES (MitoVES-F) after pretreatment of the cells with MitoTracker Red. Figure 6 shows that for proliferating ECs, MitoVES-F colocalized with MitoTracker Red, as

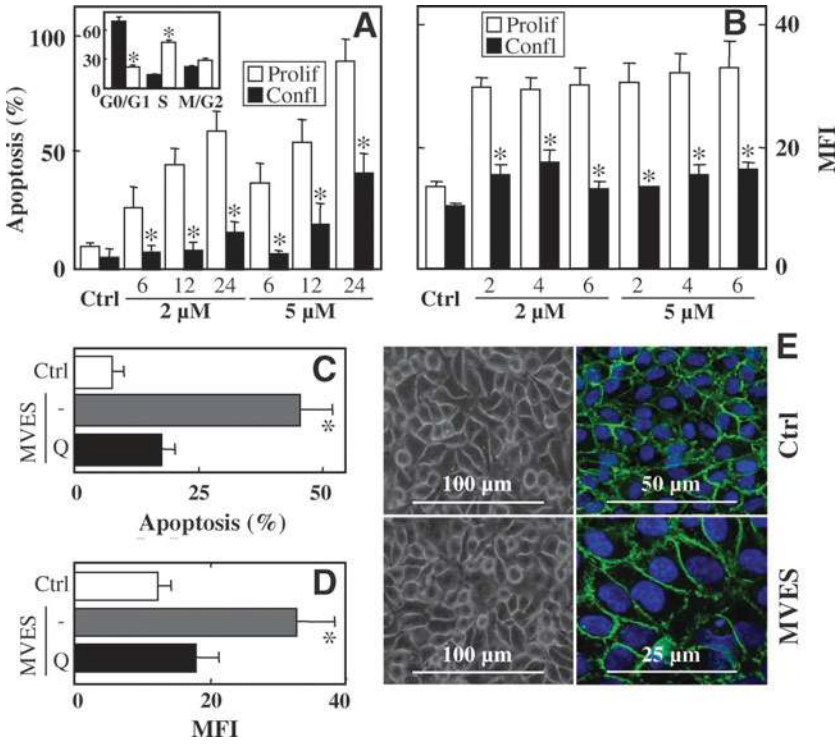

FIG. 2. MitoVES-dependent apoptosis is linked to the proliferative status of endothelial cells (ECs). EAhy926 cells plated to reach ~50% confluency (proliferating cells) and 100% confluency (confluent cells) were exposed to MitoVES at the concentrations and for the times shown. The cells were harvested and assessed for apoptosis by using annexin V-FITC/propidium iodide **(A)** and for the level of reactive oxygen species (ROS) using 2′,7′-dihydrodichlorofluorescein diacetate (DCFA) **(B)**. The *inset* in *panel* **(A)** documents the proliferative status of the cells at 50% and 100% confluency. *Panels* **(C)** and **(D)** show levels of apoptosis and ROS, respectively, in proliferating ECs preincubated with 2 μM mitochondrially targeted analog of coenzyme Q (MitoQ) and exposed to 5 μM MitoVES for 12 h **(C)** or 6 h **(D)**. **(E)** EAhy926 cells were seeded on cover slips and allowed to reach 100% confluence. After this, the cells were either left untreated (*upper panels*) or exposed for 20 h to 5 μM MitoVES (*lower panels*). The cells were then either photographed in a light microscope (*left panels*) or fixed, incubated with anticadherin VE IgG followed by secondary FITC-conjugated IgG, mounted in DAPI-containing Vectashield, and inspected in a confocal microscope. The data shown are mean values ± SD ($n = 3$), the symbol "*" indicated data from proliferating cells significantly different ($p < 0.05$) from those from arrested cells **(A, B)**, and significant differences ($p < 0.05$) in data from cells treated with MitoVES in the absence and presence of MitoQ **(C, D)**. The images in *panel* **(E)** are representative of three independent experiments. MFI, mean fluorescence intensity.

evidenced by the orange color of the organelles, documenting mitochondrial localization of the VE analog. However, we observed a rather diffuse pattern of green fluorescence in the confluent ECs which did not colocalize with the MitoTracker Red-positive structures, thus indicating that MitoVES associated much more with nonmitochondrial subcellular structures in the arrested compared with the proliferating ECs.

In the next experiments, we evaluated $\Delta\Psi_{m,i}$ in the proliferating and confluent ECs by using tetramethylrhodamine methyl ester (TMRM). We first estimated the levels of $\Delta\Psi_{m,i}$ by using confocal microscopy. Images in Figure 7A are suggestive of a higher intensity of TMRM fluorescence in the proliferating cells compared with their arrested counterparts. Further, the images indicate mitochondria in the arrested cells that appeared more round, consistent with the images in Figure 6 and those acquired by using transmission electron microscopy (TEM) (Fig. 7B). Flow cytometric analysis documented in Figure 7C reveals that $\Delta\Psi_{m,i}$ in the angiogenic cells was approximately twice the level in the arrested cells. Treatment with the uncoupler carbonyl cyanide 4-(trifluoromethoxy)phenylhydrazone (FCCP) at the concentration that completely dissipates $\Delta\Psi_{m,i}$ lowered the TMRM signal of the proliferating cells about three-fold, which is in sharp contrast to the confluent cells (Fig. 7C), where the drop in TMRM signal on FCCP addition was much more modest. To find out whether greater $\Delta\Psi_{m,i}$ is the reason for the susceptibility of angiogenic proliferating ECs to MitoVES, we tested apoptosis in the cells in the presence or absence of FCCP. Figure 7D indicates that FCCP significantly suppressed apoptosis in proliferating ECs exposed to MitoVES, whereas it had no effect on apoptosis induced by α-TOS that lacks the mitochondria-targeting cation. Inspection of lysates from confluent and arrested ECs by Native Blue electrophoresis showed virtually no difference in the assembly of the mitochondrial complexes (Fig. 7E). We next tested whether the lower $\Delta\Psi_{m,i}$ in confluent ECs, a reason for their greater resistance to MitoVES, is not potentially a result of lower number of mitochondria in confluent ECs. To do this, western blotting was performed on total cellular protein from confluent and proliferating ECs by using antibodies against subunits of complex I (CI), CII, CIII, and CV, all constituents of the MIM, as well as the mitochondrial outer membrane porin. Figure 7F reveals that the ratio of the level of the individual proteins, normalized to actin, in confluent and proliferating ECs is close to 1, thus indicating that similar or even smaller number of mitochondria are present in proliferating compared with arrested ECs. This is further supported by the activity of citrate synthase, which was 103 ± 3 and 76 ± 5 nmol/min/mg protein for confluent and proliferating ECs, respectively. We next assessed the total level of protein in proliferating and in confluent cells and found some 20% less total protein in the former. This means that per cell, proliferating cells do have considerably higher $\Delta\Psi_{m,I}$, that is, at least partially responsible for their susceptibility to MitoVES.

We earlier documented that α-TOS induces apoptosis by targeting the mitochondrial CII, which was recently crystallized (41). More specifically, we found that it interferes with the proximal (Q_P) and, most likely, too, distal ubiquinone-

binding site(s) of the protein (6, 9). We recently performed molecular modeling of the interaction of MitoVES with CII, taking into consideration the assumption that due to the positively charged TPP^+ group, the agent will be positioned so that the TPP^+ moiety will be adjacent to the matrix face of the MIM and the tocopheryl succinyl group will reach the Q_P site (7) only when the aliphatic chain of MitoVES is of sufficient length. Indeed, when we tested MitoVES homologs with 9-, 7-, or 5-C aliphatic chain (Fig. 1) in proliferating EC cells, we found that the full-length MitoVES was the most efficient one in induction of apoptosis and in suppressing angiogenesis *in vitro* using the wound-healing assay, whereas $MitoVE_5S$ exerted almost no activity (Fig. 8). These findings indicate that MitoVES relays its toxic effects on proliferating ECs by interacting with the Q_P site of CII.

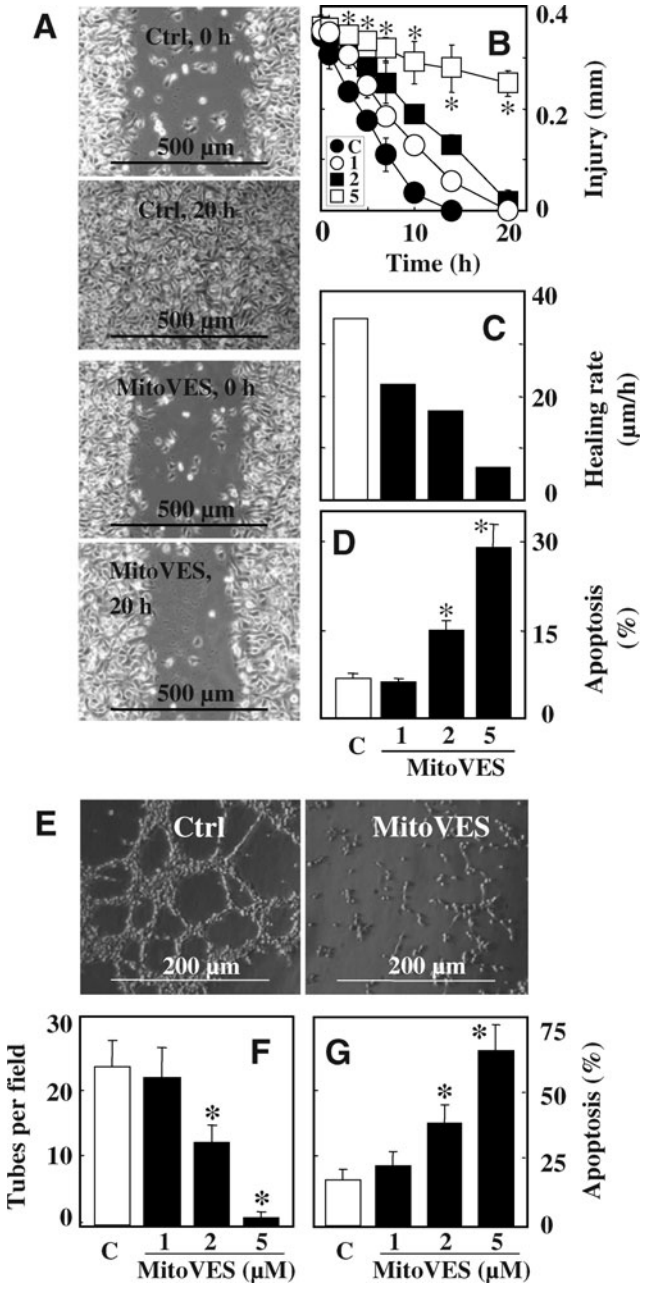

Finally, we tested the effect of MitoVES on tumor progression in a transgenic mouse with HER2-positive breast carcinomas and on angiogenesis in the carcinomas employing the ultrasound imaging (USI) technique, which allows for noninvasive and precise evaluation of the progression of tumors and their vascularization (angiogenesis). Figure 9 documents a strong inhibitory effect of the agent on the tumors including angiogenesis. Thus, in the control tumors, the relative vascularization increased some 2.5-fold over the period of the treatment, whereas it basically did not change in the treated animals. This indicates suppression of blood vessel proliferation in tumors in mice treated with MitoVES and suggests that the results on angiogenesis *in vitro* (see above) are also reflected in experimental tumors.

Discussion

The Holy Grail in the development of anticancer agents would be a compound that would interfere with the tumor cells at multiple levels and, at the same time, would leave the noncancerous somatic cells unaffected. In addition, such a compound should be effective against as wide a range of various cancer types as possible, while retaining the aforementioned specificity for cancer cells. One desired exception to this specificity is the proliferating EC. Normally, ECs remain quiescent, forming the inner lining of the blood vessels. At a tumor site, this steady state is disturbed, and the quiescent ECs are induced to proliferate to participate in the formation of new blood vessels that provide the growing tumor

FIG. 3. MitoVES inhibits angiogenesis *in vitro*. For wound-healing activity assay, EAhy926 cells were seeded in culture dishes and allowed to reach complete confluency. The central part of the endothelial monolayer was wounded by removing a lane of cells ~ 0.5 mm across. Gap narrowing by proliferating and migrating cells was then followed in control cultures and in the presence of MitoVES. *Panel* **(A)** shows representative images of the dishes with ECs at time zero and 20 h in the absence or presence of 5 μM MitoVES. At different times, the gap width was assessed in the microscope and plotted as a function of time **(B)**. The "healing rate" was estimated from the slopes in *panel* **(B)** and expressed in μm/h **(C)**. The level of apoptosis in the "wounded" EAhy926 cultures was assessed at 42 h **(D)**. For the tube-forming activity assay, EAhy926 cells were seeded in 24-well plates with 300 μl of Matrigel per well so that the suspension of 200 μl of a complete medium with 5×10^5 cells were added to each well, and incubated in the absence or presence of MitoVES. *Panel* **(E)** shows micrographs of tubes formed in 12 h in the absence or presence of 5 μM MitoVES. The number of tubes in control cultures as well as those supplemented with MitoVES at concentrations shown (μM) was evaluated by counting the number of complete tubes connecting the points of individual polygons of the capillary network at 24 h as detailed in Materials and Methods section **(F)**. Cells were retrieved after 24 h from Matrigel and assessed for the level of apoptosis **(G)**. The micrographs in *panels* **(A)** and **(E)** are representative images of three independent experiments. The data in *panels* **(B)**, **(D)**, **(F)** and **(G)** are mean values $\pm$ SD ($n = 3$). The symbol "*" in *panel* **(B)** denotes statistically significant difference of samples treated with the different concentrations of MitoVES form the controls, whereas in *panels* **(D)**, **(F),** and **(G),** it denotes statistically significant differences from the controls ($p < 0.05$).

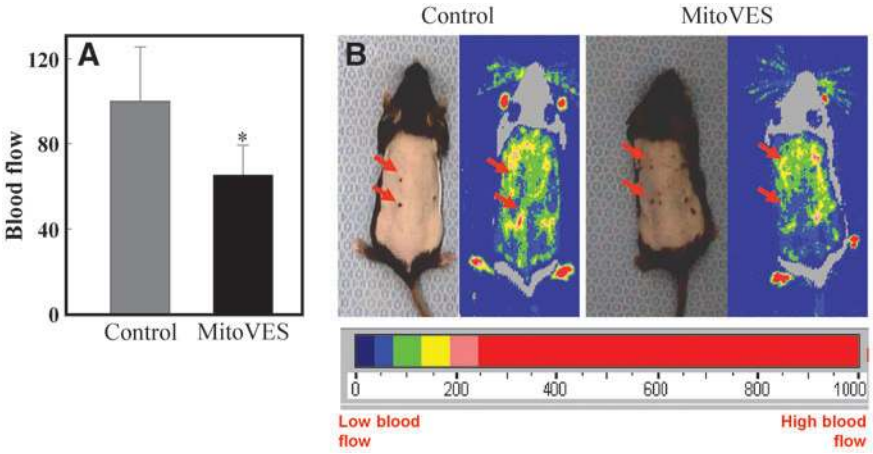

FIG. 4. MitoVES inhibits angiogenesis *in vivo*. Mice were wounded (*red arrows* indicate the wound positions) and treated with daily doses of 20 μM MitoVES in EtOH or identical volume of the excipient (control) for up to 7 days. On day 7, blood flow was visualized and quantified by a Lazer Doppler blood perfusion imager. **(A)** The data (blood flow), **(B)** representative images of the animals. The data shown are mean values ± SD ($n = 3$), the images are representative of three independent experiments. The symbol "*" denotes statistically significant differences from the controls ($p < 0.05$).

with nutrition and oxygen (13). This process, known as angiogenesis, is universal for all solid tumors, and its attenuation is considered beneficial and widely applicable to cancer treatment (14).

Potentially useful compounds in this regard are VE analogs, such as α-TOS and its mitochondrially-targeted derivative MitoVES that we recently developed. With regard to α-TOS, we already documented that it not only eliminates cancer cells but also proliferating ECs and inhibits angiogenesis (10, 33). We now show that the mitochondrial targeting of MitoVES by the TPP^+ group greatly enhances the effectivity of the parental, nontargeted compound and results in efficient killing of proliferating ECs already at concentrations as low as 2 μM, while discriminating between proliferating and arrested ECs. This would allow much lower therapeutic doses to be effectively used, which is preferential with regard to potential off-target effects. Selectivity for killing of angiogenic ECs was shown also for 4-(N-(S-glutathionylacetyl)amino) phenylarsenoxide, an arsenite analog, that was reported to induce apoptosis in proliferating ECs by interfering with the mitochondrial adenine nucleotide translocator (5).

It is apparent that MitoVES induces cell death in proliferating ECs by a mechanism similar to or identical with the parental, nontargeting α-TOS, which involves the increase of ROS before apoptosis induction as well as inhibition of angiogenesis in our models (10). This process is inhibited by the mitochondrially targeted antioxidant MitoQ and does not take place in the ECs with nonfunctional mitochondria, as shown using the ρ^0 EAhy926 cells. The shortening of the aliphatic linker between the succinate and the TTP^+ group also results in decreased activity of MitoVES, consistent with the requirement for the succinyl group to reach the ubiquinone-binding sites of mitochondrial CII, which has been shown to be the target through which α-TOS induces apoptosis in cancer cells (6, 9). This evidence shows that mitochondrial targeting using a linker of the right length between the targeting and the effector group is a plausible approach to increase effectivity of VE analogs while preserving the same or similar molecular mechanism, whereas the short-linker compounds lose effectivity, as their bioactive group cannot reach the target. Further downstream events, although not studied here, are likely to be mechanistically similar to those induced by α-TOS and MitoVES in cancer cells, where oxidative stress induced by the agents causes activation of the Hippo/Mst1 kinase, activation of the transcription factor FoxO1, and the subsequent increase in the expression of the Noxa protein, ultimately resulting in the generation of Bak-dependent channels in the mitochondrial outer membrane (8, 34, 44). Thus, since mitochondrial targeting also makes MitoVES an efficient and selective cancer cell killer (7), this modification produces an anticancer compound that promises to target tumors at multiple levels (direct tumor cell elimination and

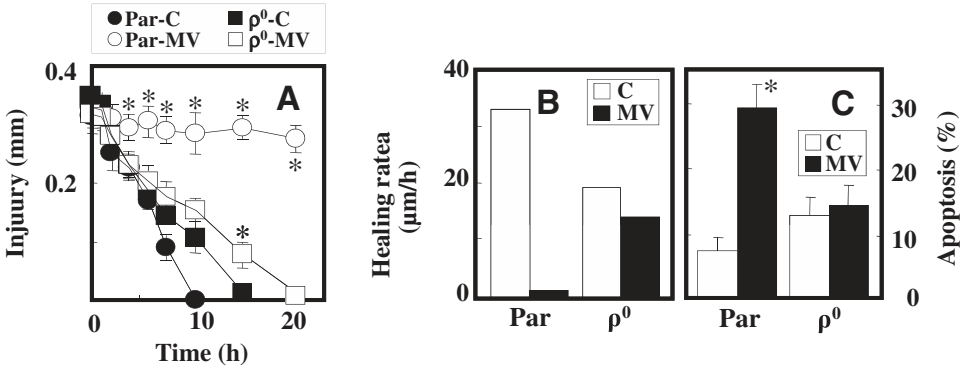

FIG. 5. ECs depleted of mtDNA are resistant to MitoVES. Proliferating parental and ρ^0 ECs were seeded in Petri dishes, allowed to reach confluency, and the endothelium was wounded. Regrowth was followed in the absence or presence of 5 μM MitoVES for up to 20 h, and the wound-healing activity expressed as the width of the wound as the function of time **(A)** and in μm/h **(B)** as detailed in Materials and Methods section. At the end of the experiment (20 h), the individual cultures were assessed for the level of apoptosis. The data in *panels* **(A)** and **(C)** are mean values ± SD. ($n = 3$). The symbol "*" denotes statistically significant differences between control and treated cells.

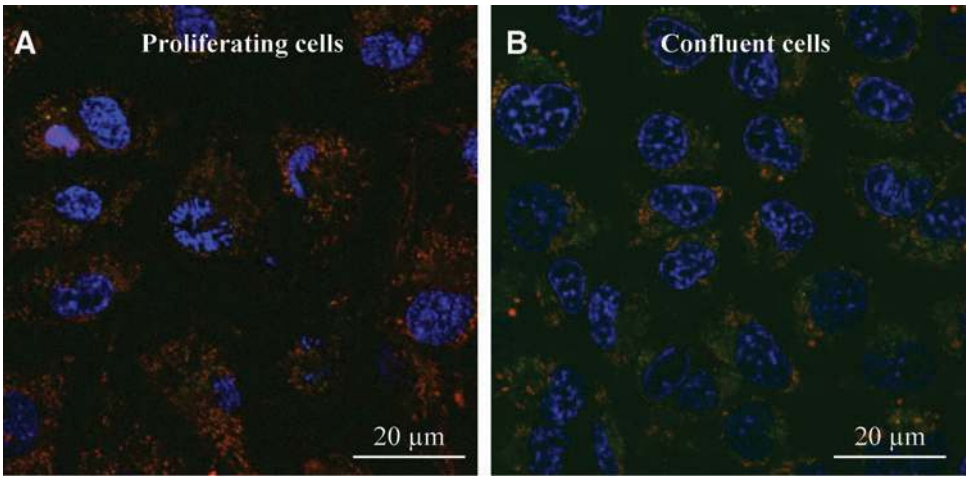

FIG. 6. MitoVES localizes to mitochondria. Proliferating **(A)** and confluent **(B)** EAhy926 cells were exposed to fluorescently tagged MitoVES (MitoVES-F) (green) at 10 μM for 30 min, after addition of MitoTracker Red and the Hoechst 33342 nuclear dye (blue), and live cells were inspected for green (MitoVES-F), red (MitoTracker Red), and blue fluorescence (Hoechst). The images are representative of 3 independent experiments.

angiogenesis inhibition) and with high efficiency and specificity, fulfilling the criteria for effective and broadly applicable anticancer agents.

Mitochondrial targeting of MitoVES is important for the observed high efficiency in killing proliferating ECs. This is exemplified by the propensity of fluorescently labeled MitoVES to accumulate in the mitochondria of proliferating ECs. In contrast, this accumulation was much less evident in confluent ECs, which are resistant to MitoVES-induced apoptosis. This suggests that mitochondrial uptake of MitoVES may be different in proliferating and confluent ECs. With regard to this, ECs represent a very interesting model that allows us to study the factors which determine MitoVES effectiveness and selectivity. Although MitoVES also displays preference for killing cancer cells as opposed to normal nontransformed cells, these represent different cell types harboring great differences in various cellular components. In contrast, it can be assumed that proliferating and confluent ECs are essentially identical in basic characteristics, and the factors associated with differences in susceptibility to MitoVES can be uncovered by using the cells at these two distinct proliferation states.

This article identifies that (at least) one major contributor to the difference in susceptibility of proliferating and arrested ECs to MitoVES is the considerable alteration in the mitochondrial potential ($\Delta\Psi_{m,i}$) of the two states of the cells. We show here, for the first time, that ($\Delta\Psi_{m,i}$) is higher in the proliferating ECs compared with confluent counterparts. That cells with greater $\Delta\Psi_{m,i}$ are susceptible to the killing activity of MitoVES is logical, given the notion that mitochondrial targeting of compounds tagged with the TPP^+ group is dependent on $\Delta\Psi_{m,i}$. Without relatively high $\Delta\Psi_{m,i}$, it is not possible for MitoVES to accumulate inside mitochondria. This is supported by the observation that the uncoupler FCCP, which dissipates $\Delta\Psi_{m,i}$, interferes with the induction of apoptosis by MitoVES, but not by the untargeted parental compound α-TOS. We have observed a similar paradigm also for cancer cells, which failed to undergo apoptosis when exposed to MitoVES in the presence of FCCP (7).

It should be noted that the difference in $\Delta\Psi_{m,i}$ is unlikely to be the sole factor that makes proliferating ECs susceptible to apoptosis induction by MitoVES. The nontargeted α-TOS also displays preference for eliminating proliferating ECs, albeit with much lower efficacy requiring the use of substantially higher concentrations for the desired effect to become apparent (10). Further research that is beyond the scope of this study will be necessary to elucidate these additional factors. For now, suffice to say that, given the safety of mitochondrial delivery by lipophilic TPP^+ accentuated by phase I/II trials with MitoQ-containing TPP^+ used for treatment of neurological disorders and hepatitis with no adverse effects even after more than 1 year of supplementation (17, 39), with MitoVES, we have an agent available that, besides specifically killing cancer cells (7), efficiently eliminates proliferating ECs while leaving the arrested confluent ECs unaffected. As such, MitoVES possesses a set of interesting biological properties that allow it to attack cancer simultaneously at several fronts and, in the future, turn the odds of cancer treatment in the patient's favor. This notion is epitomized by the profound effect of MitoVES on the tumor progression and inhibition of angiogenesis. We propose that given the anticancer effect of MitoVES due to selective killing of tumor cells (7, 8) and inhibiting tumorigenic angiogenesis (this report), clinical tests are warranted, taking into consideration the inhibitory effect of MitoVES on wound healing. To this end, MitoVES is one of very few compounds that have been reported to selectively kill proliferating but not arrested ECs, which endows it with a substantial clinical spin.

Materials and Methods

Cell culture and reagents

The endothelial-like EAhy926 cells (11) were maintained in DMEM supplemented with 10% fetal calf serum and antibiotics, plus HAT (100 μM hypoxanthine, 0.4 μM aminopterin, and 16 μM thymidine). These cells retain properties of ECs, including expression of factor VIII (11), tube-forming activity, and the propensity to persist in confluent cultures (1). EAhy926 cells deficient in mtDNA (ρ^0 phenotype) were prepared as detailed elsewhere (46). Acquisition of the ρ^0 phenotype was confirmed by the lack of expression of the mtDNA-coded cytochrome c oxidase subunit II but not its nDNA-coded subunit IV (data not shown). The proliferating and confluent ECs were used in the various experiments such that a similar number of cells was assessed.

The cells were treated under conditions of proliferation (40%–50% confluency) or arrest (100% confluency), in most cases with MitoVES, a compound with an 11-carbon linker joining the tocopheryl succinyl head group and the

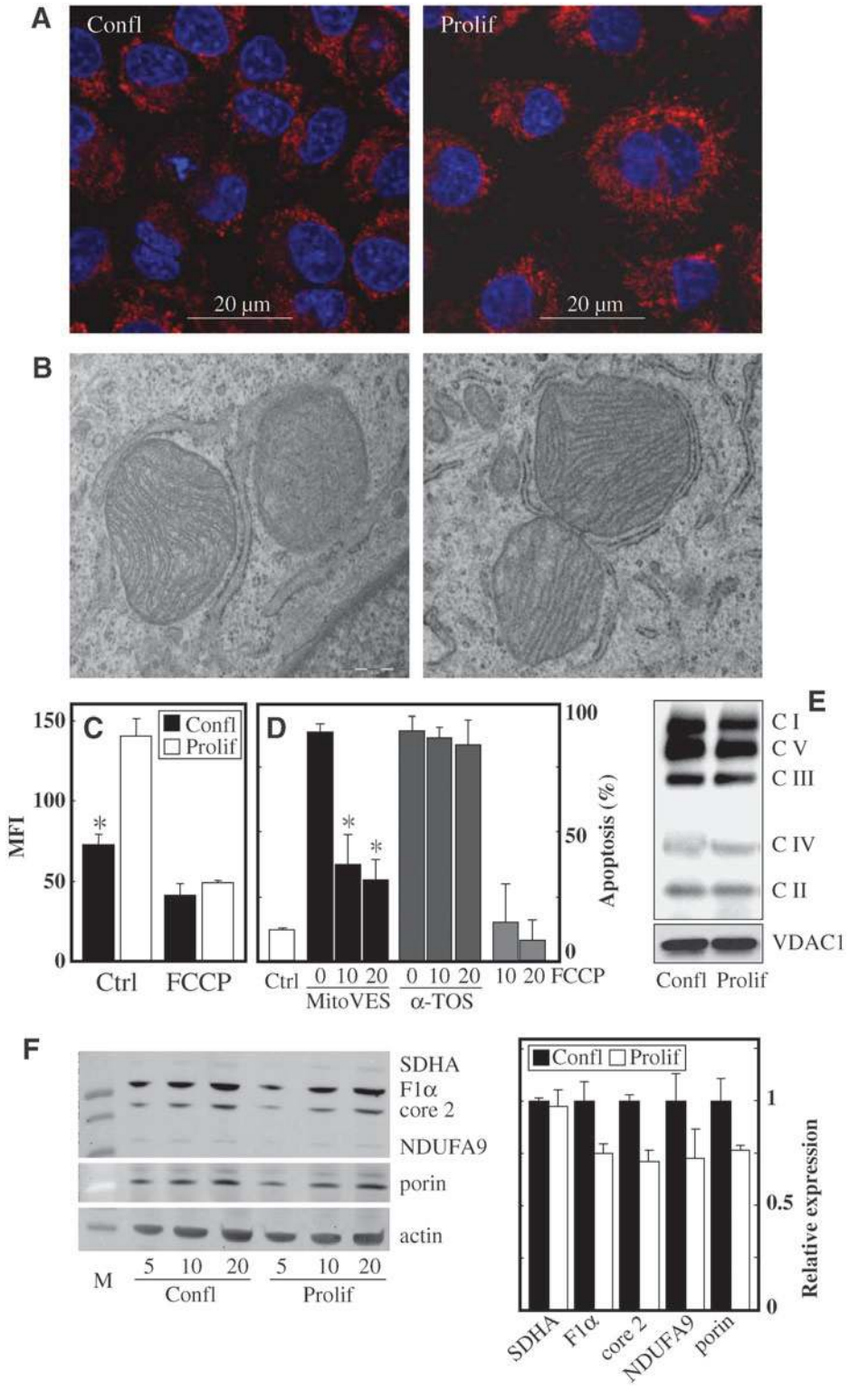

FIG. 7. Susceptibility of proliferating ECs to MitoVES is based on their higher mitochondrial potential. (A) Confluent (*left*) and proliferating (*right*) EAhy926 cells were supplemented with tetramethylrhodamine methyl ester (TMRM), the nuclei were stained with the Hoechst 33342 dye, and live cells were inspected by confocal microscopy. **(B)** Proliferating and confluent EAhy926 cells were fixed, sectioned, and inspected for mitochondrial morphology by transmission electron microscopy. **(C)** Proliferating and confluent EAhy926 cells were incubated with TMRM in the absence or presence of carbonyl cyanide 4-(trifluoromethoxy)-phenylhydrazone (FCCP), and the relative mitochondrial potential assessed by flow cytometry. **(D)** Proliferating EAhy926 cells were exposed to 5 μM MitoVES for 9 h in the presence or absence of FCCP at the concentrations shown (μM) and the level of apoptosis assessed. **(E)** Proliferating and confluent EAhy926 cells were subjected to Native Blue electrophoresis to visualize the individual mitochondrial complexes. VDAC1 was used as the loading control. **(F)** Cellular extract from confluent and proliferating ECs was subjected to SDS-PAGE followed by western blotting (*left panel*) using antibodies to subunits of complex II (CII) (SDHA), CV (F1α), CIII (core 2 subunit), and CI (NDUFA9), and to the outer membrane constituent porin. Actin was used as a loading control. The *right panel* shows the ratios of the relative level of individual proteins detected by western blotting related to actin after their densitometric evaluation. Images in panel **(A, B, E,** and **F,** *left*) are representative of three independent experiments, data in *panels* **(C)** and **(D)** are mean values ± SD ($n = 3$), and data in *panel* **(F)** (*right*) are average values ± SD derived from the densitograpic evaluation of the level of the different proteins obtained with three different amounts of total protein loaded **(**c.f. *panel* **F**, *left***)**. The symbol "*" denotes statistically significant differences between the control and treated cells ($p < 0.05$).

mitochondria-targeting TPP^+ group (Fig. 1). We also exposed ECs to VES4TPP, a compound derived from α-TOS, in which the TPP^+ group is attached to the free carboxyl group of the succinyl moiety *via* a 4-carbon linker, as well as to shorter-chain homologs of MitoVES (Fig. 1). To show mitochondrial localization, a fluorescent analog of MitoVES (MitoVES-F; for structure see Fig. 1) was prepared by addition of 5-aminofluorescein to the free carboxylate of MitoVES. The detailed description of the synthesis of the mitochondrially targeted compounds shown in Figure 1 will be published separately.

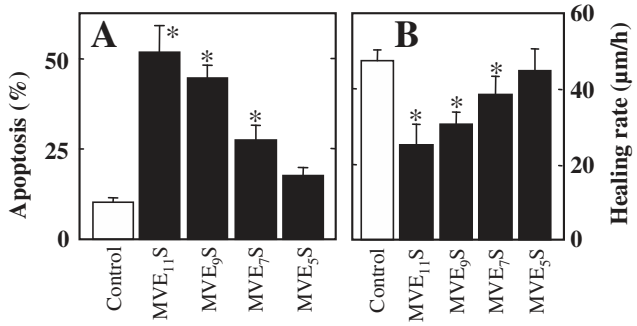

FIG. 8. Susceptibility of ECs to MitoVES is dependent on its structure. (A) EAhy926 cells at 50%–60% confluency were exposed to MitoVES homologs with different length of the aliphatic chain at 5 μM for 12 h, after which the cells were assessed for the level of apoptosis. **(B)** Fully confluent EAhy926 cells were "injured," and their re-growth followed in the presence of different MitoVES homologs at 5 μM. The "healing rate" was evaluated as detailed in Materials and Methods section. The data are mean values ± SD ($n = 3$), and the symbol "*" denotes statistically significant differences between the control and treated cells ($p < 0.05$).

Assessment of generation of intracellular ROS

Intracellular ROS levels were assessed by using the fluorescent dye 2'7'-dichlorofluorescein diacetate (DCFA). ECs were seeded in 24-well flat-bottom plates, treated, re-suspended in PBS, and supplemented with 5 μM DCFA, a cell-permeable, ROS-sensitive dye. After a 30-min incubation in the dark, the cells were collected, washed, and analyzed by flow cytometry (FACS Calibur; Becton Dickinson). The level of ROS was detected as fluorescence intensity and expressed as fold change with regard to the control.

Assessment of apoptosis and cell cycle

Apoptosis was quantified by using the annexin V-FITC method, which detects phosphatidyl serine externalized in the early phases of apoptosis (28, 46). After exposure to various compounds, floating and attached cells were collected, washed with PBS, re-suspended in 100 μl binding buffer, incubated for 20 min at room temperature with 2 μl annexin V-FITC plus 10 μl propidium iodide (PI) (10 μg/ml), and analyzed by flow cytometry by using channel 1 for annexin V-FITC binding and channel 2 for PI staining. Cell cycle was assessed as reported elsewhere (28).

Assessment of $\Delta\Psi_{m,i}$

To assess the mitochondrial membrane potential ($\Delta\Psi_{m,i}$), we used the $\Delta\Psi_{m,i}$-sensitive fluorescent probe TMRM (Sigma) at 50 nM, followed by flow cytometry assessment of red fluorescence of the mitochondria-accumulated probe. The mitochondrial uncoupler carbonyl cyanide 4-(trifluoromethoxy)-phenylhydrazone (FCCP; Sigma) was used as a control to determine nonspecific TMRM loading. The amounts of cells for various conditions were kept similar.

Native Blue electrophoresis

Confluent and proliferating EAhy926 cells were harvested by tripsinization, and the cells were resuspended in the Tris/EGTA buffer containing 200 mM sucrose and homogenized on ice with glass homogenizer at 1600 rpm. Mitochondria were isolated by differential centrifugation as follows. Lyzed cells were first centrifuged at 900 g for 10 min, and the mitochondria-containing supernatant was spun down by centrifugation at 7000 g for 15 min. Mitochondria were solubilized in the extraction buffer (1.5 M aminocaproic acid, 50 mM Bis-Tris, 0.5 M EDTA, and pH 7) containing 1.3% lauryl maltoside. Samples comprising 30–60 μg of protein were then mixed with the sample buffer (0.75 M aminocaproic acid, 50 mM Bis-Tris, 0.5 M EDTA, pH 7, 5% Serva-Blue G-250, and 12% glycerol) and loaded on the precasted NativePAGE Novex 4%–6% Bis-Tris gels run overnight at a constant voltage of 25 V. Separated protein complexes were then transferred to the PVDF membrane using the Transblot Invitrogen system. CI, CV, and CIII were detected with the Mitoprofile total OXPHOS blue native antibody coctail (MitoSciences MS 603), CIV was detected with the MTCO1 (ID6) antibody (Abcam AB14705-100), and CII was detected with the SDHA (2E3) antibody (Abcam AB14715-200).

Western blotting and citrate synthase assay

The relative number of mitochondria in the proliferating and confluent ECs was estimated by using SDS-PAGE (37) followed by western blotting using a cocktail of monoclonal antibodies against the following mitochondrial subunits: NDUFA9 subunit of CI, SDHA subunit of CII, UQCRC2 (core 2) subunit of CIII and ATP5A1 (F1α) subunit of CV (Mitosciences), and polyclonal antibody against porin/VDAC1 (4). Monoclonal antibody against actin (Calbiochem) was used as a loading control. The membranes were incubated with secondary antibodies labeled with Alexa Fluor 680 or 780 (Invitrogen; 1:3000), and the fluorescence was detected by using the Odyssey Imager (LI-COR) and quantified using the Aida 3.21 Image Analyzer software (Raytest).

The activity of the mitochondrial matrix enzyme citrate synthase was spectrophotometrically determined as described elsewhere (38).

Cadherin VE expression

For immunofluorescence microscopy, EAhy926 cells at 100% confluence were incubated with anticadherin VE IgG followed by secondary FITC-conjugated IgG and mounted with DAPI-containing Vectashield. The cells were inspected by using a confocal microscope.

Assay of mitochondrial localization of MitoVES

For the acquisition of the localization of MitoVES, the fluorescently tagged compound (MitoVE$_{11}$S-F, green) was synthesized as will be published elsewhere. EAhy926 cells were grown on cover slips (at either 50%–60% or 100% confluency), stained with the nuclear dye Hoechst 33342 (blue), MitoTracker Red (Molecular Probes), and incubated with 10 μM MitoVES-F for 30 min, after which they were inspected by using a confocal microscope.

Wound healing and tube-forming activity assessment

ECs were seeded and cultured to complete confluence. The central region of a monolayer of cells was "wounded" by scraping away cells, generating a denuded 0.5-mm wide stripe. Re-growth of cells was assessed by following the kinetics of filling the gap, visualized under a microscope

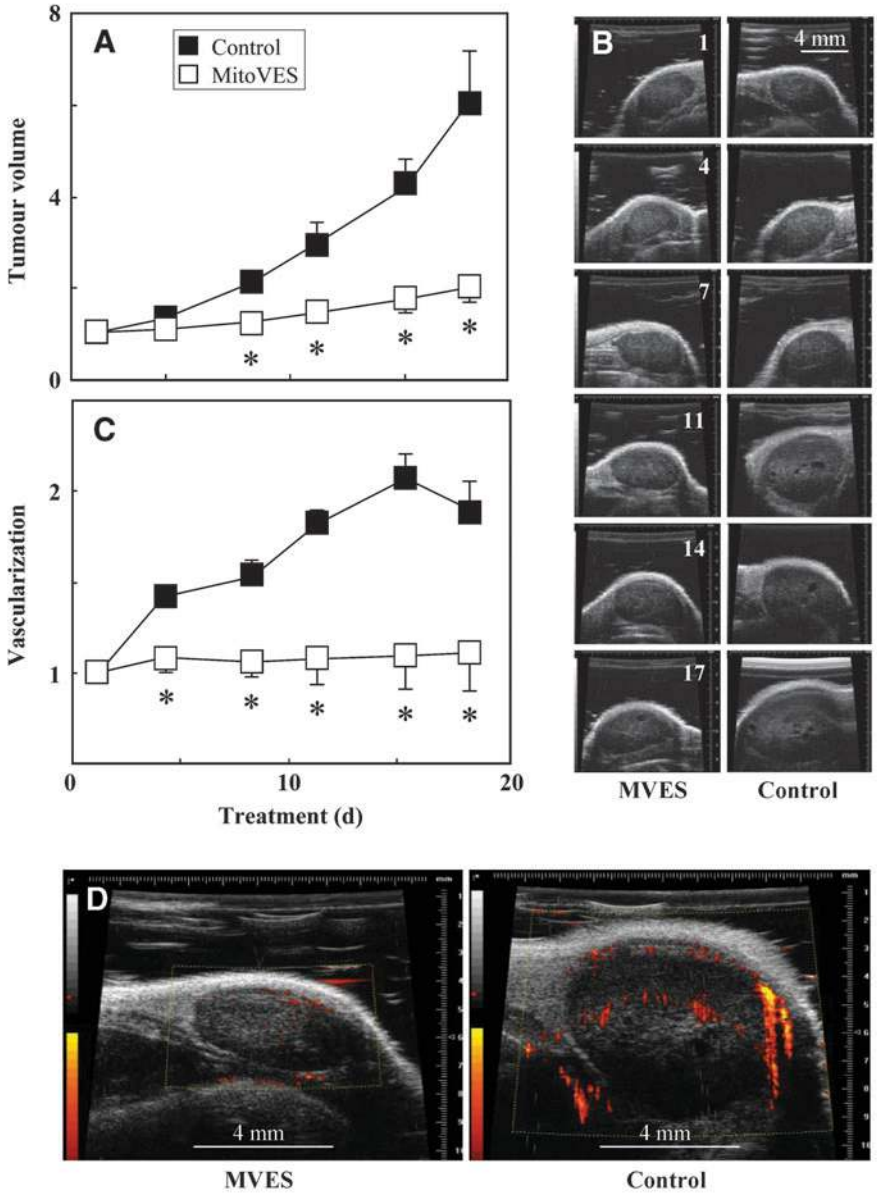

FIG. 9. MitoVES suppresses tumor progression and angiogenesis in a mouse model. Female FVB/N *c-neu* mice with small tumors ($\sim 40\,mm^3$) were treated by intraperitoneal injection twice a week with 100 μl 6 m*M* MitoVES in corn oil with 4% EtOH. Ultrasound imaging was used to noninvasively monitor and quantify tumor progression **(**relative volume, **A)** and tumor vascularization **(C)**. *Panel* **(B)** shows a representative tumor of treated and control mice on the individual days of the experiment, *panel* **(D)** vascularization (2D ultrasonograph) of a representative tumor of the treated and control mouse on day 17. The data in *panels* **(A)** and **(C)** are mean values ± SD ($n = 6$), and the symbol "*" denotes statistically significant differences between the control and treated animals ($p < 0.05$).

equipped with a grid in the eyepiece. The healing rate was expressed in μm/h.

For the tube-forming activity of ECs, formation of capillary-like structures in a 3-D setting was assessed, essentially as described elsewhere (11). Briefly, 300 μl of cold Matrigel (BD Biosciences) per well was transferred with a cold tip by using a 24-well plate. Matrigel was overlaid with a suspension of EAhy926 cells so that a total of 200 μl of complete media with 5×10^5 cells was added to each well. After 6 h in the incubator, the polygonal structures, made by a network of EAhy926 capillaries, were established. The cells were treated, and the tube-forming activity was estimated by counting the number of complete capillaries connecting individual points of the polygonal structures in a light microscope 24 h after transferring the cells onto Matrigel. Three fields in the central area were randomly chosen in every well. The number of capillaries in control cultures was considered 100%.

Assessment of wound healing in vivo

The mouse *in vivo* model of wound healing was essentially used as described (36), employing the MoorLDI-Mark 2 lazer Doppler blood perfusion imager (Moore Instruments Ltd.) (2). C57BL/6 mice between the ages of 8 and 10 weeks were used. The back of the mouse was shaved with standard animal hair clippers (No. 40 blade) and disinfected with betadine. Using microdissecting forceps, the skin of the animal was lifted along the line as shown, and a 4-mm dermal biopsy punch was driven through the two folds of skin. MitoVES was dissolved in EtOH and applied at the final concentration of 20 μM. Control mice received an identical volume of EtOH. On day 1, 10 μl of the drug or the excipient were applied at 4 points surrounding the wound *via* an inward injection. On day 2 and onward, the drug was topically applied through the tegaderm dressing. The images were acquired on day 7.

Transmission electron microscopy

Cells were subjected to TEM after being processed as described (46).

Animal tumor studies

Transgenic FVB/N202 *c-neu* mice carrying the rat HER2/neu proto-oncogene driven by the MMTV promoter on the H-2^q FVB/N background (19) were established at the Griffith University Animal Facility and maintained under strict inbreeding conditions. About 70% of the female mice develop spontaneous mammary carcinomas with a mean latency time of 10 months (6–12 months). Female FVB/N202 rat *c-neu* mice with small tumors (about 40 mm^3) were treated with either 100 μl 6 m*M* MitoVES in 4% ethanol/corn oil or the same volume of the excipient by intraperitoneal injection once every 3 or 4 days. Tumor volume and relative vascularization were quantified by using the Power Doppler Mode of the USI instrument (the Vevo770 device fitted with the RMV704 scanhead from VisualSonics) twice a week after each treatment. Both the treated and the control group contained at least 6 mice. Mouse body temperature and the setting of the Power Doppler mode were kept the same throughout the experiment.

All animal experiments were performed according to the guidelines of the Australian and New Zealand Council for the Care and Use of Animals in Research and Teaching and were approved by the Griffith University Animal Ethics Committee.

Statistical analysis

All data shown are mean values of three independent experiments (unless stated otherwise) ± SD. Statistical significance was assessed by using Student's *t*-test, and differences were considered significant at $p < 0.05$. For animal experiments, the difference in the mean relative tumor size ± SEM was examined by using analyses of covariance (ANCOVA) with days as the covariate. Statistical analyses were performed by using SPSS® 10.0 analytical software (SPSS). Differences were considered statistically significant when the value of $p < 0.05$.

Acknowledgments

This project was supported in part by grants from the Australian Research Council, the National Health and Medical Research Council of Australia, the Cancer Council Queensland, the Grant Agency of the Czech Republic (204/08/0811, 305/07/1008, P301/10/1937) and the Grant Agency of the Academy of Sciences of the Czech Republic (KAN200520703) to J.N., the National Institutes of Health (NS42617, GM77185, and GM69589) to C.K.S, and the Ministry of Education, Youth and Sports of the Czech Republic (1M6837805002) to J.H. The authors thank Ivana Novakova for technical assistance.

Author Disclosure Statement

The authors disclose no conflict of interest.

References

1. Albini A, Marchisone C, Del Grosso F, Benelli R, Masiello L, Tacchetti C, Bono M, Ferrantini M, Rozera C, Truini M, Belardelli F, Santi L, and Noonan DM. Inhibition of angiogenesis and vascular tumor growth by interferon-producing cells: a gene therapy approach. *Am J Pathol* 156: 1381–1393, 2000.
2. Biswas S, Roy S, Banerjee J, Hussain SR, Khanna S, Meenakshisundaram G, Kuppusamy P, Friedman A, and Sen CK. Hypoxia inducible microRNA 210 attenuates keratinocyte proliferation and impairs closure in a murine model of ischemic wounds. *Proc Natl Acad Sci U S A* 107: 6976–6981, 2010.
3. Cross MJ and Claesson-Walsh L. FGF and VEGF function in angiogenesis: signalling pathways, biological responses and therapeutic inhibition. *Trends Pharmacol Sci* 22: 201–207, 2001.
4. De Pinto V, Prezioso G, Thinnes F, Link TA, and Palmieri F. Peptide-specific antibodies and proteases as probes of the transmembrane topology of the bovine heart mitochondrial porin. *Biochemistry* 30: 10191–10200, 1991.
5. Don AS, Kisker O, Dilda P, Donoghue N, Zhao X, Decollogne S, Creighton B, Flynn E, Folkman J, and Hogg PJ. A peptide trivalent arsenical inhibits tumor angiogenesis by perturbing mitochondrial function in angiogenic endothelial cells. *Cancer Cell* 3: 497–509, 2003.
6. Dong LF, Freeman R, Liu J, Zobalova R, Marin-Hernandez A, Stantic M, Rohlena J, Rodriguez-Enriquez S, Valis K, Butcher B, Goodwin J, Brunk UT, Witting PK, Moreno-Sanchez R, Scheffler IE, Ralph SJ, and Neuzil J. Suppression of tumour growth *in vivo* by the mitocan α-tocopheryl succinate requires respiratory complex II. *Clin Cancer Res* 15: 1593–1600, 2009.
7. Dong LF, Jameson VJA, Tilly D, Cerny J, Mahdavian E, Marín-Hernández A, Hernández-Esquivel L, Rodríguez-Enríquez S, Witting PK, Stantic B, Rohlena J, Truksa J, Kluckova K, Dyason JC, Salvatore BA, Moreno-Sánchez R, Coster MJ, Ralph SJ, Smith RAJ, and Neuzil J. Mitochondrial targeting of vitamin E succinate enhances its pro-apoptotic and anti-cancer activity via mitochondrial complex II. *J Biol Chem* 286: 3717–3728, 2011.
8. Dong LF, Jameson VJA, Tilly D, Prochazka L, Rohlena J, Valis K, Truksa J, Zobalova R, Mahdavian E, Kluckova K, Stantic M, Stursa J, Wang XF, Freeman R, Witting PK, Norberg E, Goodwin J, Salvatore BA, Novotna J, Turanek J, Ledvina M, Hozak P, Zhivotovsky B, Coster MJ, Ralph SJ, Smith RAJ, and Neuzil J. Mitochondrial targeting of α-tocopheryl succinate enhances its pro-apoptotic efficacy: A new paradigm of efficient anti-cancer therapy. *Free Radic Biol Med* 50: 1546–1555, 2011.
9. Dong LF, Low P, Dyason J, Wang XF, Prochazka L, Witting PK, Freeman R, Swettenham E, Valis K, Liu J, Zobalova R, Turanek J, Spitz DR, Domann FE, Scheffler IE, Ralph SJ, and Neuzil J. α-Tocopheryl succinate induces apoptosis by targeting ubiquinone-binding sites in mitochondrial respiratory complex II. *Oncogene* 27: 4324–4335, 2008.
10. Dong LF, Swettenham E, Eliasson J, Wang XF, Gold M, Medunic Y, Stantic M, Low P, Prochazka L, Witting PK, Turanek J, Akporiaye ET, Ralph SJ, and Neuzil J. Vitamin E analogs inhibit angiogenesis by selective apoptosis induction in proliferating endothelial cells: The role of oxidative stress. *Cancer Res* 67: 11906–11913, 2007.
11. Edgell CJ, McDonald CC, and Graham JB. Permanent cell line expressing human factor VIII-related antigen established by hybridization. *Proc Natl Acad Sci U S A* 80: 3734–3737, 1983.
12. Fantin VR and Leder P. Mitochondriotoxic compounds for cancer therapy. *Oncogene* 5: 4787–4797, 2006.
13. Folkman J. Angiogenesis. *Annu Rev Med* 57: 1–18, 2006.

14. Folkman J. Angiogenesis: an organizing principle for drug discovery? *Nat Rev Drug Discov* 6: 273–286, 2007.
15. Folkman J and Shing Y. Angiogenesis. *J Biol Chem* 267: 10931–10934, 1992.
16. Fulda S, Galluzzi L, and Kroemer G. Targeting mitochondria for cancer therapy. *Nat Rev Drug Discov* 9: 447–464, 2010.
17. Gane EJ, Orr DW, Keogh GF, Gibson M, Lockhart MM, Frampton CM, Taylor KM, Smith RA, and Murphy MP. The mitochondria-targeted anti-oxidant mitoquinone decreases liver damage in a phase II study of hepatitis C patients. *Liver Int* 30: 1019–1026, 2010.
18. Gogvadze V, Orrenius S, and Zhivotovsky B. Mitochondria in cancer cells: what is so special about them? *Trends Cell Biol* 18: 165–173, 2008.
19. Guy CT, Webster MA, Schaller M, Parsons TJ, Cardiff RD, and Muller WJ. Expression of the neu protooncogene in the mammary epithelium of transgenic mice induces metastatic disease. *Proc Natl Acad Sci U S A* 89: 1078–1082, 1992.
20. Jemal A, Siegel R, Ward E, Hao Y, Xu J, and Thun MJ. Cancer statistics, 2010. *CA Cancer J Clin* 60: 277–300, 2010.
21. Kelso GF, Porteous CM, Coulter CV, Hughes G, Porteous WK, Ledgerwood EC, Smith RA, and Murphy MP. Selective targeting of a redox-active ubiquinone to mitochondria within cells: antioxidant and antiapoptotic properties. *J Biol Chem* 276: 4588–4596, 2001.
22. Malafa MP, Fokum FD, Andoh J, Neitzel LT, Bandyopadhyay S, Zhan R, Iiizumi M, Furuta E, Horvath E, and Watabe K. Vitamin E succinate suppresses prostate tumor growth by inducing apoptosis. *Int J Cancer* 118: 2441–2447, 2006.
23. Malafa MP, Fokum FD, Mowlavi A, Abusief M, and King M. Vitamin E inhibits melanoma growth in mice. *Surgery* 131: 85–91, 2002.
24. Moreno-Sánchez R, Rodríguez-Enríquez S, Marín-Hernández A, and Saavedra E. Energy metabolism in tumor cells. *FEBS J* 274: 1393–1418, 2007.
25. Murphy MP and Smith R. Targeting antioxidants to mitochondria by conjugation to lipophilic cations. *Annu Rev Pharmacol Toxicol* 47: 629–656, 2007.
26. Neuzil J. Vitamin E succinate and cancer treatment: a vitamin E prototype for selective anti-tumour activity. *Br J Cancer* 89: 1822–1826, 2003.
27. Neuzil J, Dong LF, Ramanathapuram L, Hahn T, Chladova M, Wang XF, Zobalova R, Prochazka L, Gold M, Freeman RE, Turanek J, Akporiaye ET, Dyason J, and Ralph SJ. Vitamin E analogues: a novel group of mitocans, anti-cancer agents that act by targeting mitochondria. *Mol Aspects Med* 28: 607–645, 2007.
28. Neuzil J, Schröder A, von Hundelshausen P, Zernecke A, Weber T, Gellert N, and Weber C. Inhibition of inflammatory endothelial responses by a pathway involving caspase activation and p65 cleavage. *Biochemistry* 40: 4686–4692, 2001.
29. Neuzil J, Swettenham E, Wang XF, Dong LF, and Stapelberg M. α-Tocopheryl succinate inhibits angiogenesis by disrupting paracrine FGF2 signalling. *FEBS Lett* 581: 5611–5615, 2007.
30. Neuzil J, Tomasetti M, Zhao Y, Dong LF, Birringer M, Wang XF, Low P, Wu K, Salvatore BA, and Ralph SJ. Vitamin E analogs, a novel group of 'mitocans', as anti-cancer agents: The importance of being redox-silent. *Mol Pharmacol* 71: 1185–1199, 2007.
31. Neuzil J, Wang XF, Dong LF, Low P, and Ralph SJ. Molecular mechanism of 'mitocan'-induced apoptosis in cancer cells epitomizes the multiple roles of reactive oxygen species and Bcl-2 family proteins. *FEBS Lett* 580: 5125–5129, 2006.
32. Neuzil J, Weber T, Gellert N, and Weber C. Selective cancer cell killing by α-tocopheryl succinate. *Br J Cancer* 84: 87–89, 2001.
33. Park D and Dilda P. Mitochondria as targets in angiogenesis inhibition. *Mol Asp Med* 31: 113–131, 2010.
34. Prochazka L, Dong LF, Valis K, Freeman R, Ralph SJ, Turanek J, and Neuzil J. α-Tocopheryl succinate causes mitochondrial permeabilization by preferential formation of Bak channel. *Apoptosis* 15: 782–794, 2010.
35. Rafii S, Lyden D, Benezra R, Hattori K, and Heissig B. Vascular and haematopoietic stem cells: novel targets for anti-angiogenesis therapy? *Nat Rev Cancer* 2: 826–835, 2002.
36. Roy S, Biswas S, Khanna S, Gordillo G, Bergdall V, Green J, Marsh CB, Gould LJ, and Sen CK. Characterization of a preclinical model of chronic ischemic wound. *Physiol Genomics* 37: 211–224, 2009.
37. Schägger H and von Jagow G. Tricine-sodium dodecyl sulfate-polyacrylamide gel electrophoresis for the separation of proteins in the range from 1 to 100 kDa. *Anal Biochem* 166: 368–379, 1987.
38. Singh M, Brooks GC, and Srere PA. Subunit structure and chemical characteristics of pig heart citrate synthase. *J Biol Chem* 245: 4636–4640, 1970.
39. Snow BJ, Rolfe FL, Lockhart MM, Frampton CM, O'Sullivan JD, Fung V, Smith RA, Murphy MP, and Taylor KM. A double-blind, placebo-controlled study to assess the mitochondria-targeted antioxidant MitoQ as a disease-modifying therapy in Parkinson's disease. *Mov Disord* 25: 1670–1674, 2010.
40. Stapelberg M, Gellert N, Swettenham E, Tomasetti M, Witting PK, Procopio A, and Neuzil J. α-Tocopheryl succinate inhibits malignant mesothelioma by disrupting the FGF autocrine loop: the role of oxidative stress. *J Biol Chem* 280: 25369–25376, 2005.
41. Sun F, Huo X, Zhai Y, Wang A, Xu J, Su D, Bartlam M, and Rao Z. Crystal structure of mitochondrial respiratory membrane protein complex II. *Cell* 121: 1043–1057, 2005.
42. Tomasetti M, Gellert N, Procopio A, and Neuzil J. A vitamin E analogue suppresses malignant mesothelioma in a preclinical model: a prototype of a future drug against a fatal neoplastic disease? *Int J Cancer* 109: 641–642, 2004.
43. Trachootham D, Alexandre J, and Huang P. Targeting cancer cells by ROS-mediated mechanisms: a radical therapeutic approach? *Nat Rev Drug Discov* 8: 579–591, 2009.
44. Valis K, Prochazka L, Boura E, Chladova M, Obsil T, Rohlena J, Truksa J, Dong LF, Ralph SJ, and Neuzil J. Hippo/Mst1 stimulates transcription of *NOXA* in a FoxO1-dependent manner. *Cancer Res* 71: 946–954, 2011.
45. Wang XF, Birringer M, Dong LF, Veprek P, Low P, Swettenham E, Stantic M, Yuan LH, Zobalova R, Wu K, Ralph SJ, Ledvina M, and Neuzil J. A peptide adduct of vitamin E succinate targets breast cancer cells with high erbB2 expression. *Cancer Res* 67: 3337–3344, 2007.
46. Weber T, Dalen H, Andera L, Nègre-Salvayre A, Augé N, Sticha M, Loret A, Terman A, Witting PK, Higuchi M, Plasilova M, Zivny J, Gellert N, Weber C, and Neuzil J. Mitochondria play a central role in apoptosis induced by α-tocopheryl succinate, an agent with anticancer activity. Comparison with receptor-mediated pro-apoptotic signaling. *Biochemistry* 42: 4277–4291, 2003.

47. Weber T, Lu M, Andera L, Lahm H, Gellert N, Fariss MW, Korinek V, Sattler W, Ucker DS, Terman A, Schröder A, Erl W, Brunk U, Coffey RJ, Weber C, and Neuzil J. Vitamin E succinate is a potent novel anti-neoplastic agent with high tumor selectivity and cooperativity with tumor necrosis factor-related apoptosis-inducing ligand (TRAIL, Apo2L) *in vivo*. *Clin Cancer Res* 8: 863–869, 2002.

Address correspondence to:
Prof. Jiri Neuzil
School of Medical Science
Griffith University
Southport QLD 4222
Australia

E-mail: j.neuzil@griffith.edu.au

Dr. Lan-Fang Dong
School of Medical Science
Griffith University
Southport QLD 4222
Australia

E-mail: l.dong@griffith.edu.au

Dr. Jakub Rohlena
Institute of Biotechnology
Academy of Sciences of the Czech Republic
Prague 142 20
Czech Republic

E-mail: jakub.rohlena@img.cas.cz

Date of first submission to ARS Central, July 26, 2011; date of final revised submission, August 29, 2011; date of acceptance, August 30, 2011.

Abbreviations Used

α-TOS = α-tocopheryl succinate
$\Delta\Psi_{m,i}$ = mitochondrial inner trans-membrane potential
CI = complex I
DCFA = 2′,7′-dihydrodichlorofluorescein diacetate
ECs = endothelial cells
FCCP = carbonyl cyanide 4-(trifluoromethoxy) phenylhydrazone
MIM = mitochondrial inner membrane
MitoQ = mitochondrially targeted analog of coenzyme Q
MitoVES = mitochondrially targeted analog of α-tocopheryl succinate
MitoVES-F = fluorescently tagged MitoVES
PI = propidium iodide
Q_P = proximal ubiquinone-binding site
ROS = reactive oxygen species
TEM = transmission electron microscopy
TMRM = tetramethylrhodamine methyl ester
TPP^+ = triphenyl phosphonium
USI = ultrasound imaging
VE = vitamin E